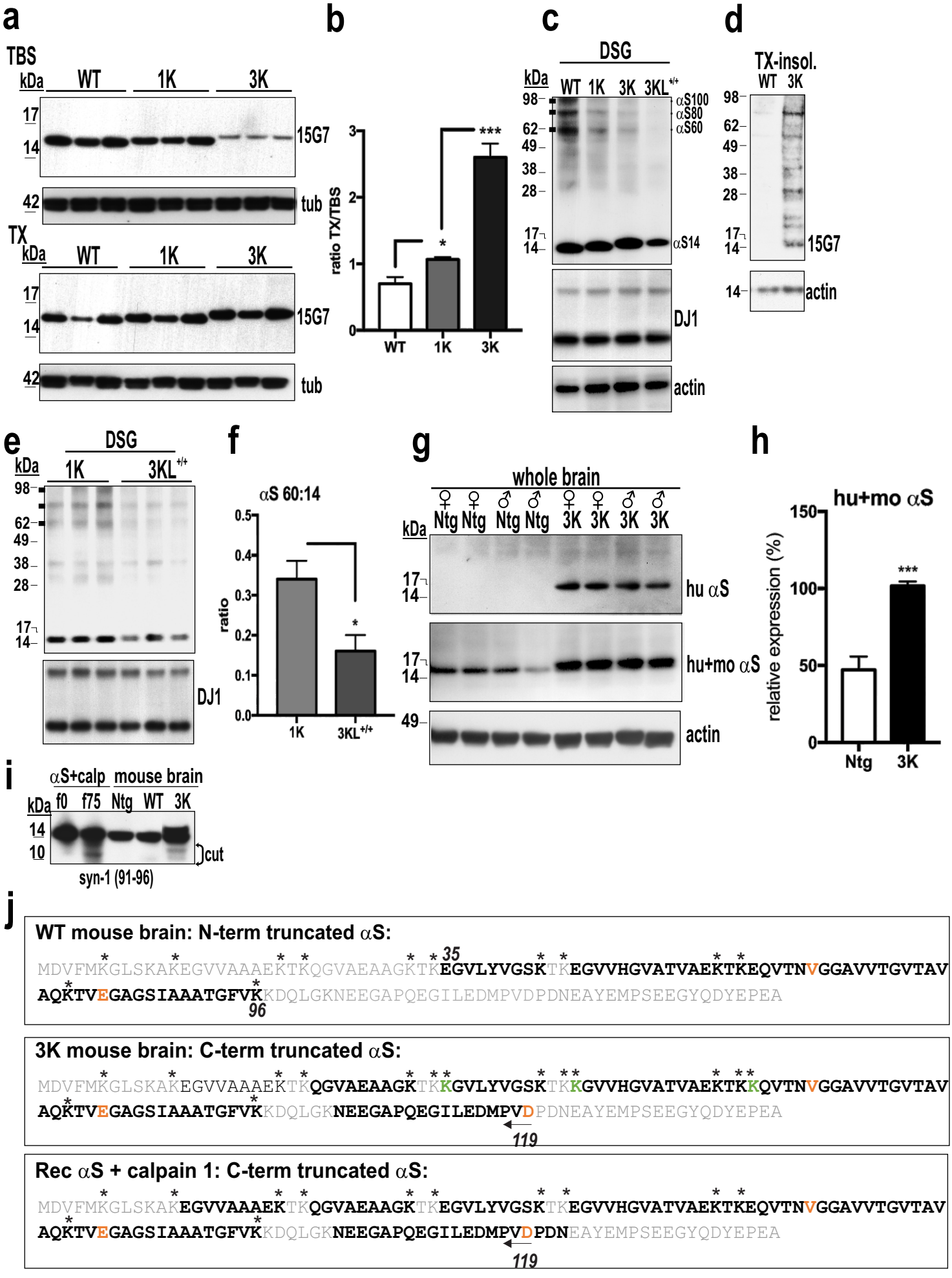
a
TBS
kDa
WT
1K
3K
17
14
15G7
42
tub
TX
kDa
WT
1K
3K
17
14
15G7
42
tub
b
ratio TX/TBS
3
2
1
0
*
***
WT
1K
3K
c
DSG
kDa
WT 1K 3K 3KL+/+
98
62
49
38
28
17
14
αS100
αS80
αS60
αS14
DJ1
actin
d
TX-insol.
WT 3K
98
62
49
38
28
17
14
15G7
14
actin
e
DSG
kDa
1K
3KL+/+
98
62
49
38
28
17
14
DJ1
f
αS 60:14
ratio
0.5
0.4
0.3
0.2
0.1
0.0
*
1K
3KL+/+
g
whole brain
♀ ♀ ♂ ♂ ♀ ♀ ♂ ♂
Ntg Ntg Ntg Ntg 3K 3K 3K 3K
kDa
17
14
hu αS
hu+mo αS
49
actin
h
hu+mo αS
relative expression (%)
150
100
50
0
***
Ntg
3K
i
αS+calp
mouse brain
kDa
f0
f75
Ntg
WT
3K
14
10
cut
syn-1 (91-96)
j
WT mouse brain: N-term truncated αS:
MDVFMKGLSKAKEGVVAAAEKTKQGVAEAAGKTKEGVLYVGSKTKEGVVHGVATVAEKTKEQVTNVGGAVVTGVTAV
AQKTVEGAGSIAAATGFVKKDQLGKNEEGAPQEGILEDMPVDPDNEAYEMPSEEGYQDYEPEA
35
96
3K mouse brain: C-term truncated αS:
MDVFMKGLSKAKEGVVAAAEKTKQGVAEAAGKTKKGVLYVGSKTKKGVVHGVATVAEKTKKQVTNVGGAVVTGVTAV
AQKTVEGAGSIAAATGFVKKDQLGKNEEGAPQEGILEDMPVDPDNEAYEMPSEEGYQDYEPEA
119
Rec αS + calpain 1: C-term truncated αS:
MDVFMKGLSKAKEGVVAAAEKTKQGVAEAAGKTKEGVLYVGSKTKEGVVHGVATVAEKTKEQVTNVGGAVVTGVTAV
AQKTVEGAGSIAAATGFVKKDQLGKNEEGAPQEGILEDMPVDPDNEAYEMPSEEGYQDYEPEA
119

Figure S1

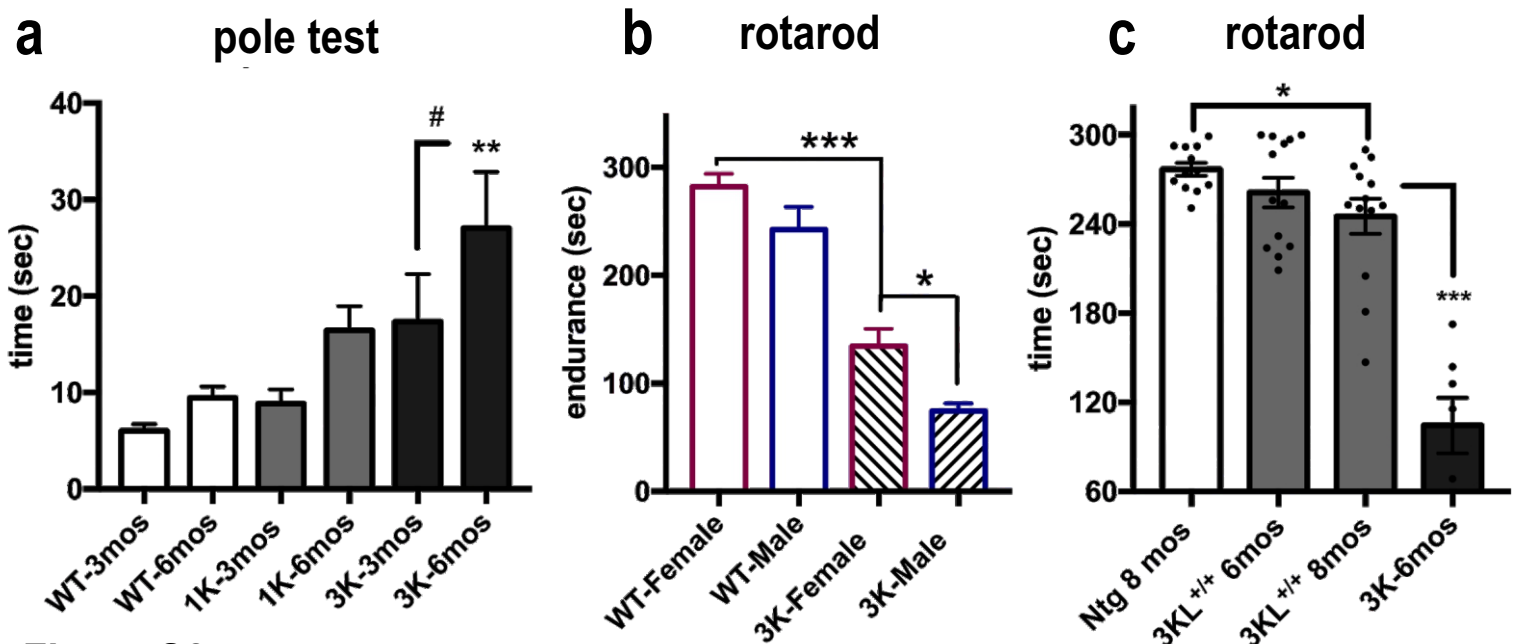
a
pole test
time (sec)
40
30
20
10
0
#
**
WT-3mos
WT-6mos
1K-3mos
1K-6mos
3K-3mos
3K-6mos
b
rotarod
endurance (sec)
300
200
100
0
***
*
WT-Female
WT-Male
3K-Female
3K-Male
c
rotarod
time (sec)
300
240
180
120
60
*
***
Ntg 8 mos
3KL+/+ 6mos
3KL+/+ 8mos
3K-6mos

Figure S2

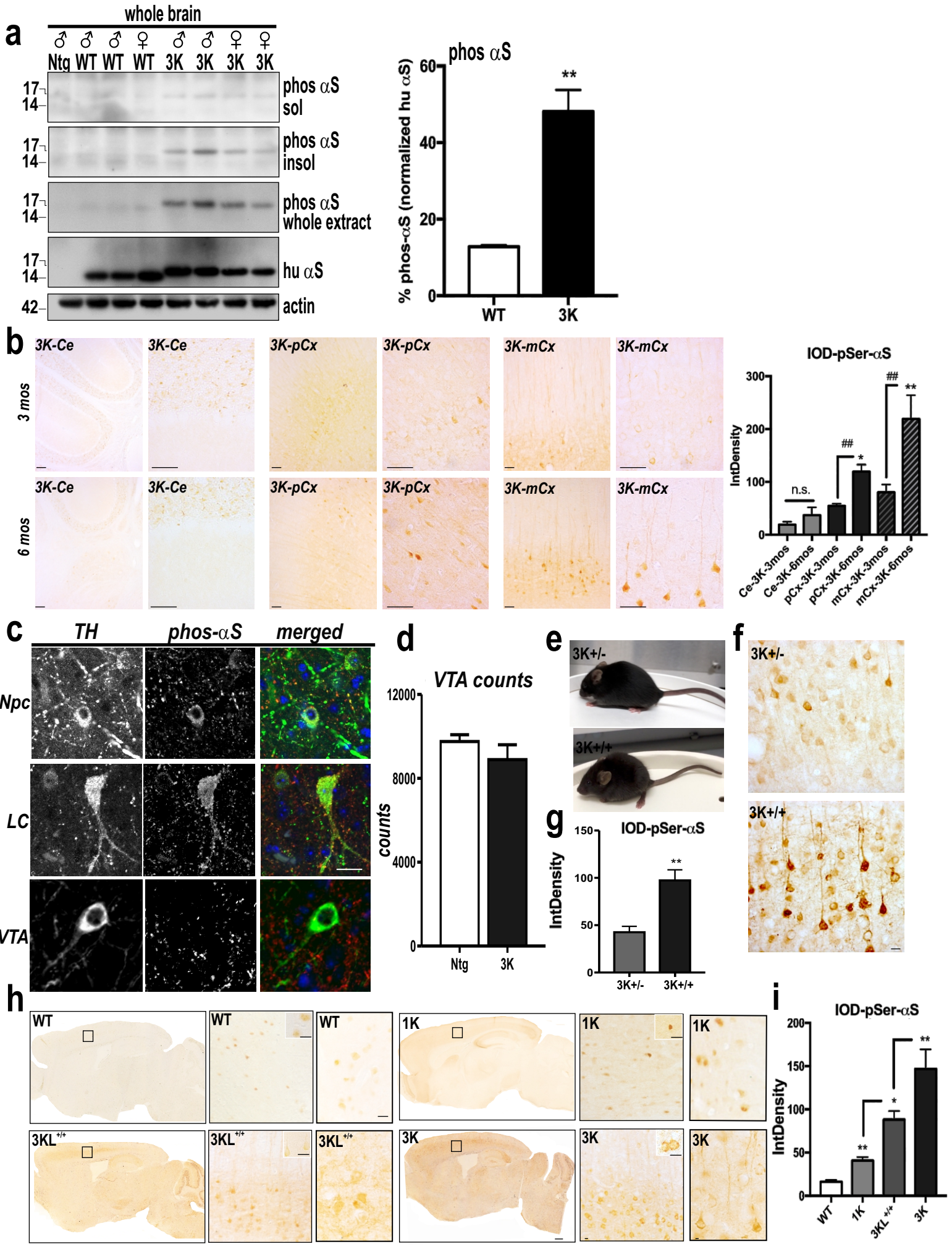
a
whole brain
♂ ♂ ♂ ♀ ♂ ♂ ♀ ♀
Ntg WT WT WT 3K 3K 3K 3K
17
14
phos αS sol
phos αS insol
phos αS whole extract
hu αS
42
actin
phos αS
% phos-αS (normalized hu αS)
60
40
20
0
**
WT
3K
b
3K-Ce
3K-pCx
3K-mCx
3 mos
6 mos
IOD-pSer-αS
IntDensity
300
200
100
0
n.s.
##
*
**
Ce-3K-3mos
Ce-3K-6mos
pCx-3K-3mos
pCx-3K-6mos
mCx-3K-3mos
mCx-3K-6mos
c
TH
phos-αS
merged
SNpc
LC
VTA
d
VTA counts
counts
12000
8000
4000
0
Ntg
3K
e
3K+/-
3K+/+
f
3K+/-
3K+/+
g
IOD-pSer-αS
IntDensity
150
100
50
0
**
3K+/-
3K+/+
h
WT
1K
3KL+/+
3K
i
IOD-pSer-αS
IntDensity
200
150
100
50
0
**
*
**
WT
1K
3KL+/+
3K

Figure S3

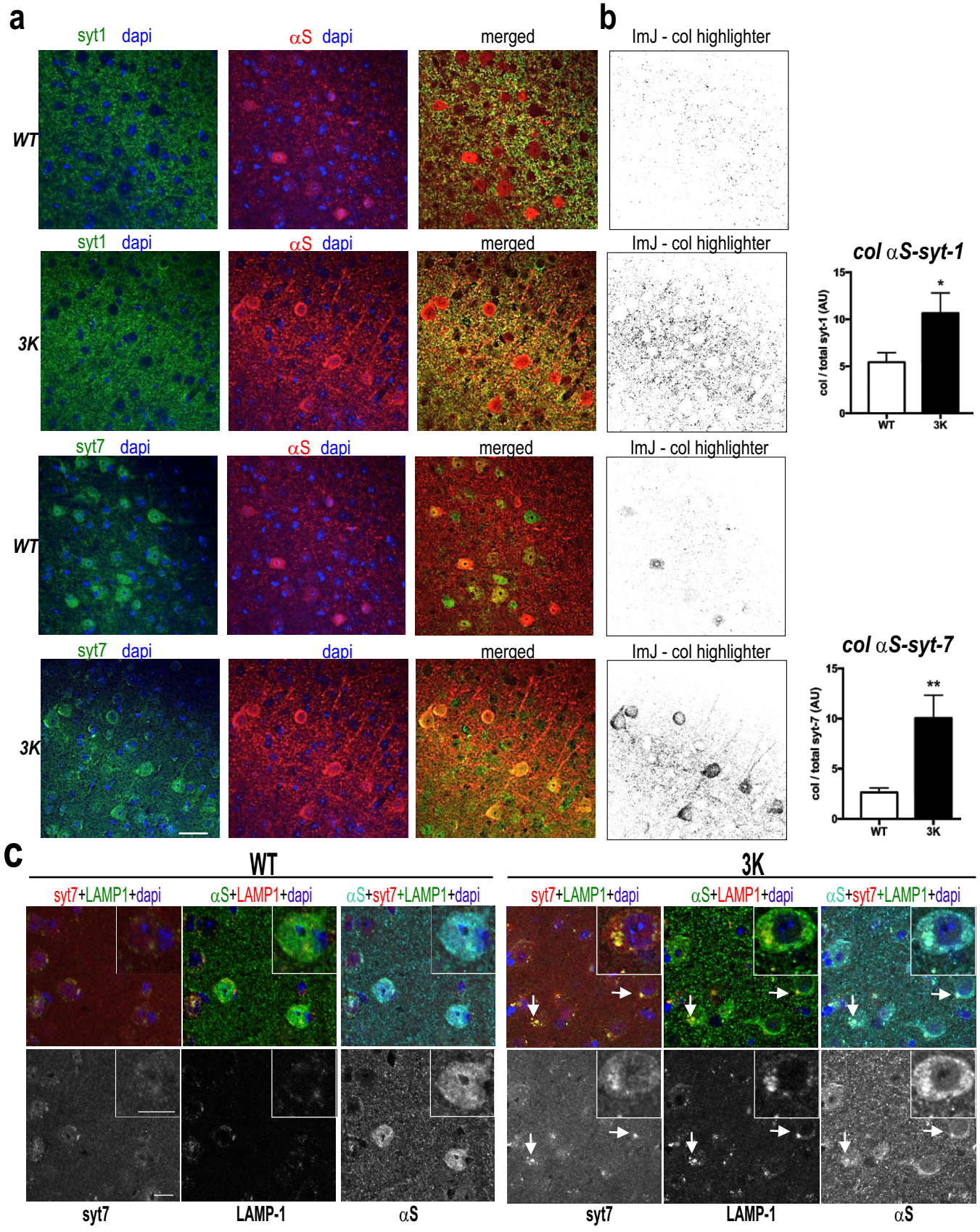
a
b
syt1 dapi
αS dapi
merged
ImJ - col highlighter
WT
3K
syt7 dapi
dapi
col αS-syt-1
col / total syt-1 (AU)
col αS-syt-7
col / total syt-7 (AU)
WT
3K
c
syt7+LAMP1+dapi
αS+LAMP1+dapi
αS+syt7+LAMP1+dapi
syt7
LAMP-1
αS

Figure S4

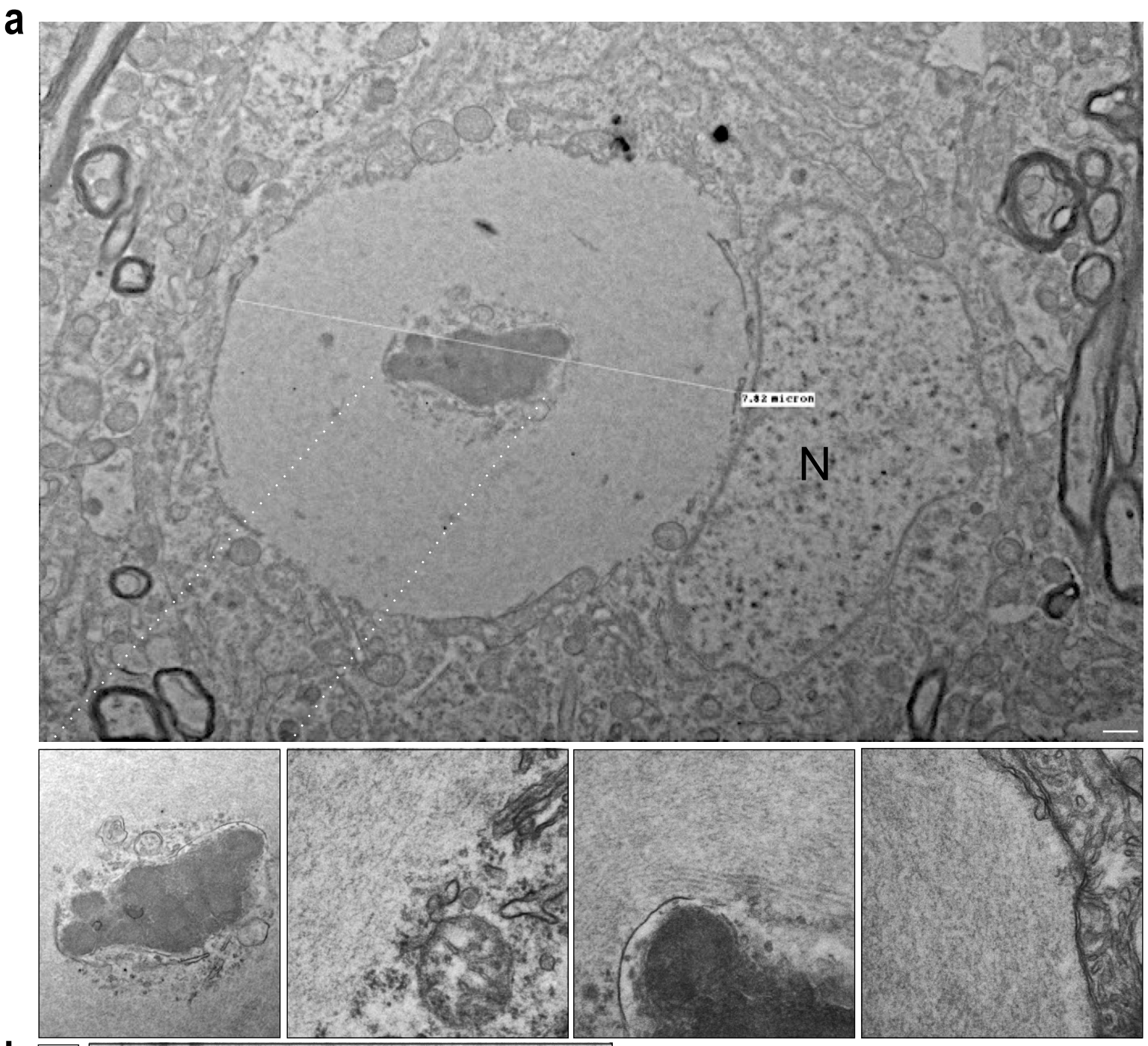
a
7.82 micron
N
b
15G7 (hu αS) post-embedding
N
c
3K-cortex
3K-midbrain

Figure S5

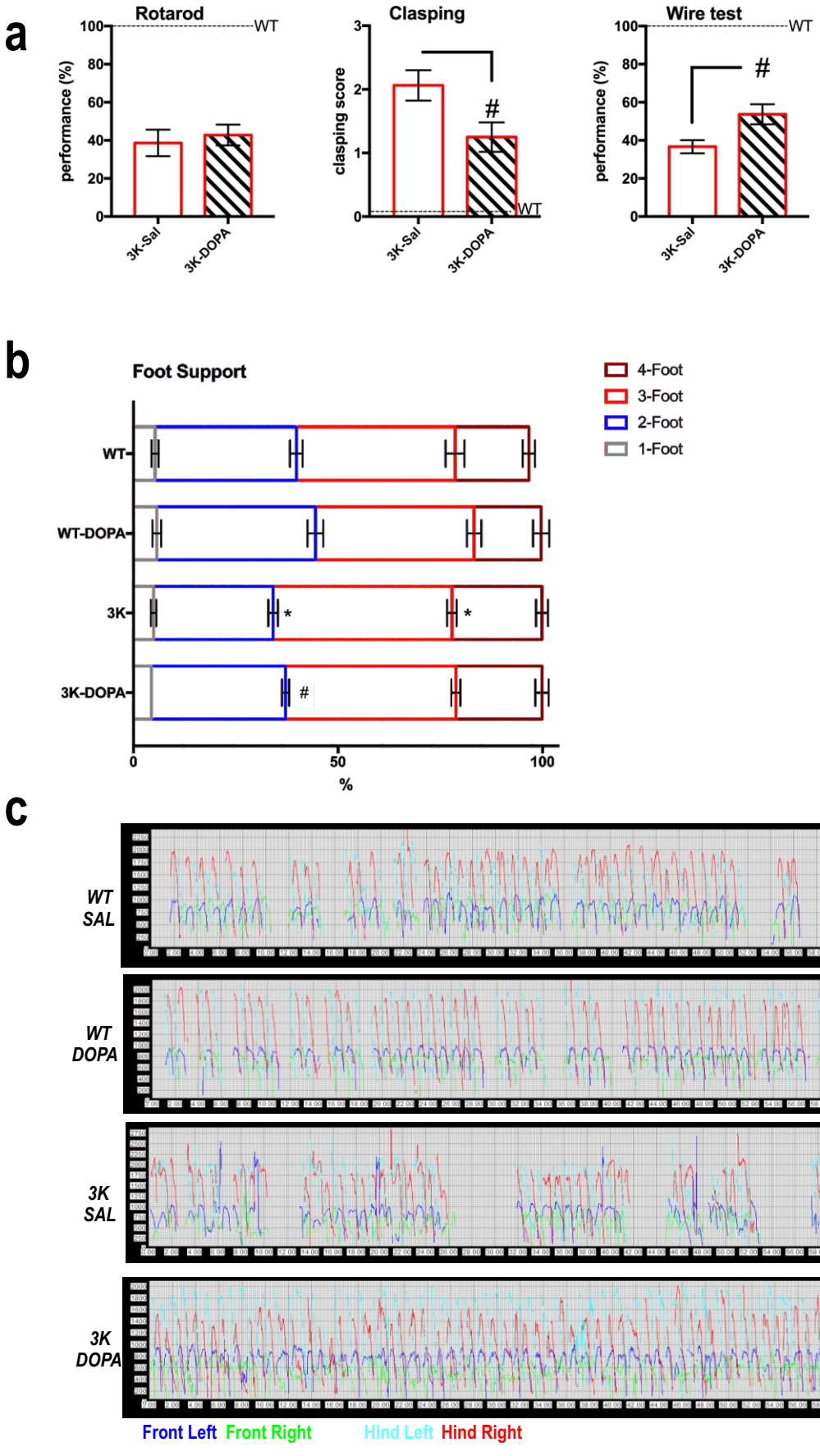
a
Rotarod
WT
performance (%)
100
80
60
40
20
0
3K-Sal
3K-DOPA
Clasping
clasping score
3
2
1
0
#
WT
Wire test
#
b
Foot Support
4-Foot
3-Foot
2-Foot
1-Foot
WT
WT-DOPA
3K
3K-DOPA
*
*
#
0
50
100
%
c
WT SAL
WT DOPA
3K SAL
3K DOPA
Front Left
Front Right
Hind Left
Hind Right

Figure S6

Supplementary Material:

Figure S1 Biochemical characterization of αS pattern in E→K mutants – related to Figure 2 (**a**) WB of sequential extractions of TBS-soluble (cytosolic) and TX-soluble (membrane) fractions of cortical homogenates (no crosslinking). (**b**) Densitometry of the bands (means ± SEM) of the same WB shows a stepwise shift from cytosol to membrane fractions in 1K and 3K vs. WT mice. (**c**) Intact-cell crosslinking of αS using the cell-penetrant crosslinker DSG on washed cortical brain bits from WT, 1K, $3KL^{+/+}$ and 3K tg mice shows tetramer-deficiency of all 3 mutant lines vs. WT. Mab syn1 detects monomeric (αS14) and tetrameric (αS60) αS and probable conformers of the tetramer (αS80, αS100). DJ-1 monomers/dimers serve as control for equal crosslinking and protein loading. (**d**) TX-insoluble fraction of cortical homogenates. (**e**) Intact-cell crosslinking of 1K vs. $3KL^{+/+}$ (n=3 each group). (**f**) Quantification of WB in (e) reveals significant decreases in T:M ratio in $3KL^{+/+}$ vs. 1K. (**g**) WB of whole brain extracts of n=4 Ntg vs. 3K mice shows ~2-fold overexpression. Hu specific 15G7 (upper panel) or C20 Mab, which detects both human and mouse αS, and (**h**) graph. (**i**) Calpain-dependent αS truncation in tetramer-deficient 3K mice: mAb Syn-1 WB of rec. fibrillized αS +/- calpain digestion (lanes 1, 2) and TBS-cytosolic homogenates of mouse cortex of 3 genotypes (lanes 3-5). Bracket: gel slices between 10-12 kDa (ΔC) were excised from lanes 4 and 5 (WT and 3K mutant mouse brains); ΔC from calpain-cleaved rec αS (lane 2) served as a positive control to guide excision and for MS. (**j**) Comparison of protein sequences derived by LC-MS/MS spectra of tryptic peptides (*black asterisks*) from the 10-12 kDa hu αS fragments of WT and 3K mouse brain and the calpain-cleaved rec. αS, using Mascot (Matrix Sciences); the detected peptides (in *boldface*) were identified by the Protein Pilot 4.0 software (Absciex). The ΔC hu αS product ending at amino acid D119 (*arrow*) was found in both 3K brain and calpain-cleaved rec. αS. The longest fragment detected in WT mouse brain spans amino acid 35 to 96. Means ± SEM. *$p < 0.05$; *** $p < 0.001$ in 1K vs. WT or 3K or $3KL^{+/+}$ vs. age- and [αS]-matched 1K; (b) one-Way ANOVA post Tukey; or (f, h) unpaired 2-tailed Student's *t* test.

Figure S2 Progressive motor deficits in tetramer-deficient αS tg mice – related to Figure 3 (**a**) Graph quantifies time to descend a pole in 3 and 6 mos WT, 1K and 3K mice (n = 6-10 males per group). (**b**) Accelerating rotarod task (4-40 rpm) reveals more severe motor deficits in 3K males than females, in comparison to their hu WT αS controls (n=5-8 per group). (**c**) Graph quantifies endurance time on rotarod in 6 and 8 mos old $3KL^{+/+}$ (homozygous 3K-Low) mice (n = 6-12 mice per group). Means ± SEM. *, $^{\#}$ $p < 0.05$; **, $^{\#\#}$ $p< 0.01$; *** $p < 0.001$ vs. age-, gender and [αS]-matched WT; one-way ANOVA, post Tukey.

Figure S3 Phosphorylated ser129-αS staining of WT and 3K mouse brain tissue – related to Figure 4. (**a**) WB of sequentially extracted (TBS-) soluble and insoluble as well as whole homogenates blotted for pSer129-αS and hu αS (15G7); densitometry of whole extracts (right) shows a ~3-fold increase of total pSer129-αS in 3K (line 3817) over WT. (**b**) Both 3 mos and 6 mos cerebellar sections display minor pSer129 signals compared to a large, age-dependent increase in pyramidal neurons of prefrontal cortex (pCx) and motor cortex (mCx) in 3K mice; quantified on right. (**c**) pSer129-αS accumulation in TH-positive neurons of the SN pars compacta (SNpc) and locus coeruleus (LC) and few dots in ventral tegmental area (VTA) in 3K brain. Scale bars. (**d**) Counts of TH+ neurons in the VTA of the midbrain. (**e**) Motor posture at rest in heterozygous $3K^{+/-}$ and homozygous $3K^{+/+}$ male mice at age 4 wk. Severe hind limb rigidity and decreased motor control in the $3K^{+/+}$ mice result in inability to sustain themselves after weaning (see Movie S7). (**f**) IHC of pSer129+ αS in sagittal brain sections from 3 mos $3K^{+/-}$ and 1 mos $3K^{+/+}$ mice. (**g**) Quantification of pSer129 optical density (n=10 fields each of cortical sections from N = 3-4 mice per

genotype). **(h)** Anti-pSer129 αS IHC of WT, 1K, 3KL$^{+/+}$ and 3K sagittal brain sections at age 6 mos. Boxes in each section indicate magnified regions shown to right. (**i**) Quant. of pSer129 optical density (n=10 fields each of cortical sections from N = 3 mice per genotype). Means ± SEM. *p < 0.05, **p < 0.01, ***p < 0.001; (a, d, g) unpaired 2-tailed Student's t test; (b, i) One-way ANOVA post Tukey. *Scale bars* (b) 50 μm (c,d,f, insets in h) 25 μm.

Figure S4 Abnormal αS accumulation at vesicles in motor cortex of 6 mos 3K mice – related to Figure 6 (**a**) Single and merged stainings show co-localization of αS with syt-1+ vesicles at synaptic terminals and with syt-7 mainly in neuronal somata. (**b**) ImageJ plug-in co-localization highlighter converts co-localized points into 8-bit greyscale images that were adjusted to a common threshold and quantified. (**c**) Confocal microscopy of sections quadruple-labeled for αS, syt-7, lysosomal-membrane associated protein-1 (LAMP-1), and nuclei (DAPI). Spectrally unmixed images are in lower panels to show large foci of αS, syt-7 and LAMP-1, and their overlap is shown in triple-merged upper panels. Means ± SEM. *p < 0.05, **p < 0.01, unpaired 2-tailed Student's t test. *Scale bars* (a) 50 μm, (c) 25 μm.

Figure S5 Ultrastructure of a cortical neuronal soma from a 16 mos old 3K male mouse – related to Figure 7. Top: (**a**) EM reveals the spherical, LB-like inclusion consists of filamentous material that is associated with a central lipofuscin deposit and membranous organelles (mainly mitochondria) along the periphery. N, nucleus. Below: Higher power EMs show a lipofuscin-rich core (far left) and (**b**) 15G7 hu αS immunogold labeling of dense filamentous deposits throughout the rest of the round inclusion. (**c**) Degenerated neurons and synapses in 3K brain. *Left*: Toluidine-blue stained semi-thin sections of cortex (upper panel) and midbrain (lower panel) show scattered neurons with dark and dense appearance of the cytoplasm and nuclear areas, shrunken cytoplasm and triangular shapes. *Right*: Dark degenerated synapses and a dark-degenerated neuron, displaying lipid deposits (white arrow) were seen. *Scale bars*: (a) top, left and bottom panel = 500nm, all other panels = 100 nm, (c-left) 20 μm, (c-right) 1 μm.

Figure S6 Gait analyses of 3K and WT mice before vs. after L-DOPA treatment – related to Figure 7. (**a**) Graphs showing L-DOPA ameliorates limb clasping and improves (lengthens) wire hanging performance, while no treatment effect occurs on the accelerating rotarod test. (**b**) Limb support graph shows L-DOPA ameliorates the elevated 3-foot and reduced 2-foot support of 3K mice. (**c**) Stance graph of the same 3K and WT mouse after saline (SAL) or L-DOPA i.p. treatment. Harmonization of the marked stance anomalies of front and hind limbs of the 3K mice upon L-DOPA treatment. Means ± SEM. *p < 0.05 WT-Sal vs. 3K-Sal; $^{\#}p$ < 0.05 3K-Sal vs. 3K-DOPA, unpaired 2-tailed Student's t test.

Table S1: Key characteristics of αS tetramers and their potential relevance to PD, related to Figures 1-7
Table S2: Mouse models of PD which express hu αS and explore L-DOPA responsive phenotypes, related to Figures 2-7

Table S2. Mouse models of PD which express hu αS and explore L-DOPA responsive phenotypes – related to Figs. 2-7

PD mutation	promoter/ zygosity	motor onset	αS inclusions		DAergic integrity			motor deficit	L-DOPA	reference
			cortex	mid-brain	SN cell loss	striatal loss	VTA			
single-mutation models										
WT	Thy-1/het	3 mos	4-5 mos	4-5 mos	none	6 mos	NR	beam slips	25 mg/kg worse	[1-3]
	CaMKIIα/het	8 mos	NR	20 mos	20 mos*	NR	NR	rotarod deficit	NR	[4]
	PDGFβ/ het	9 mos	2-3 mos	2-3 mos	none	12 mos	NR	rotarod deficit	NR	[5]
A53T	Prnp/hom	15-16 mos	sparse	none	none	none	NR	4-limb paresis	NR	[6]
	Thy-1/hom	6 mos	NR	NR	NR	NR	NR	gait, rotarod deficit	NR	[7,8]
	DAT-PF/het	none	none	1 mos	3 mos	3-12 mos	spared	none	NR	[9]
A30P	Thy-1/hom	8 mos	sparse	none	none	none	NR	rotarod deficit	NR	[10]
E46K	Prnp/hom	16-29 mos	15-19 mos	22 mos	none	none	NR	4-limb paresis	NR	[11]
	BAC/het	6 mos*	6 mos size⇧	6 mos size⇧	12mos*	NR	NR	pole deficit	NR	**present study**,[12]
LRRK-2	TH-G2019S/het	24 mos	NR	15 mos size⇧	15 mos	24 mos {DA}	NR	gait, pole deficit,	20 mg/kg improved	[13]
	R1441G-BAC/het	10-12 mos	none	none	none	10-12 mos{DA}	spared	immobility	20 mg/kg improved	[14]
multi-mutation models										
LRRK2-A53T	CaMKIIα/het	none	none	none	NR	1 mos (neuronal)	NR	hyperactivity#	none	[15]
A30P-A53T	TH/het	13-23 mos	none	none	8.5 mos	16-18 mos{DA}	NR	hypolocomotion	none	[16,17]
3K E35,46,61K	Thy-1.2/het	3 mos	3 mos size⇧	3 mos size⇧	6 mos	6 mos	spared	resting tremor, gait, pole deficit, rotarod deficit	12.5 mg/kg improved	**present study**

Abbreviation: NR, not reported. het, heterozygous. hom, homozygous. *tendency; #only A53T-dependent hyperactivity

For reference details see also main reference list : (**1**) Rockenstein et al., *J Neurosci Res,* 2002. (**2**) Fleming et al., *J Neurosci*, 2004. (**3**) Fleming et al., *Neuroscience*, 2006. (**4**) Nuber et al., *J Neurosci*, 2008. (**5**) Masliah et al., *Science*, 2000. (**6**) Giasson et al., *Neuron*, 2002. (**7**) Chandra et al., *Cell*, 2005. (**8**) Rothman et al., *J Parkinsons Dis*, 2013.(**9**) Chen et al., *J Neurosci*, 2015. (**10**) Neumann et al., *J Clin Invest*, 2002. (**11**) Emmer et al., *J Biol Chem*, 2011. (**12**) https://www.michaeljfox.org/files/MJFF_SfN_aSyn_Poster.pdf
(**13**) Xiong et al., *PNAS*, 2018. (**14**) Li et al., *Nat Neurosci*, 2009. (**15**) Lin et al., *Neuron*, 2009. (**16**) Richfield et al., *Exp Neurol*, 2002.
(**17**) Thiruchelvam et al., *Eur J Neurosci* (2004).

Table S1. Key characteristics of αS tetramers and their potential relevance to PD – related to Figs.1,2

metastable	**detected under specific conditions** • non-denaturing conditions[(a),(e),(f),(j)] • with cell-permeable crosslinkers[(a),(e),(f)] • under „molecular crowding" conditions in cell lysates[(e),(j)] • mostly found in the cytosol (TBS-soluble) fraction[(e),(f)]
not an artifact	**trapping of the native conformational state** • a non-stochastic pattern by intact-cell crosslinking (14, 60, 80, 100 kDa)[(a),(e),(f),(l),(m)] • also seen by live-cell fluorescence protein (YFP) complementation[(f),(i)]
	potential physiological function • transient vesicle association of multimers regulating neurotransmission[(h)] • cytosolic storage form resisting pathologic aggregation[(a),(d)]
non-pathologic	**abundant in native (intact-cell) healthy tissue** • freshly biopsied normal human brain[(e)] • freshly biopsied normal mouse brain (Ntg, WT)[(e),(m)] • iPSC-derived wt human neurons[(e),(l)] • can be isolated from normal human red blood cells and bacteria [(a-d)]
	shared conformation with homologues not implicated in PD • β-synuclein, γ-synuclein[(e)]
PD relevance	**Tetramer abrogation causes inclusion formation and neurotoxicity**[(f),(g),(k),(m)] **Tetramer abrogation causes pathologic modifications like those in PD** • pSer129+, ΔC-truncation, PK-resistance, relative insolubility [(m)] **Pathologic redistribution consistent with early Lewy-type changes** • abnormal membrane association, vesicle clustering[(g),(i),(k),(m)] • lysosomal alteration[(l),(m)] **PD-causing gene defects decrease the tetramer:monomer ratio in cells** • familial αS mutations (A30P, E46K, H50Q, G51D, A53T)[(f)] • Gaucher's GBA mutations lower the T:M ratio (of wt αS)[(l)] • In mice, 3x(E46K) yields PD-like αS neuropathology and L-DOPA-responsive motor signs[(m)]

For reference details, see also main reference list: (**a**) Bartels et al., *Nature*, 2011. (**b**) Wang et al., *PNAS*, 2011. (**c**) Trexler et al., *Prot Sci*, 2012. (**d**) Westphal et al., *JBC*, 2012. (**e**) Dettmer et al., *JBC*, 2013. (**f**) Dettmer et al., *Nat Commun*, 2015. (**g**) Dettmer et al., *PNAS*, 2015. (**h**) Burre et al., *PNAS*, 2014. (**i**) Wang et al., *Curr Biology*, 2014. (**j**) Luth et al., *Biochemistry*, 2015. (**k**) Dettmer et al., *Hum Mol Gen*, 2017. (**l**) Kim et al., *PNAS*, 2018.
(m) **present study**